

Supporting Information

Optical Properties Of A Sulfur-Rich ORMOCALC Polymer Synthesized Via Inverse Vulcanization And Containing An Organometallic Comonomer

Darryl A. Boyd^{1*}, Vinh Q. Nguyen¹, Collin C. McClain², Frederic H. Kung², Colin C. Baker¹, Jason D.

Myers¹, Michael P. Hunt¹, Woohong Kim¹, and Jasbinder S. Sanghera¹

¹Optical Sciences Division, Naval Research Laboratory, 4555 Overlook Ave SW, Washington, DC 20375, USA

²University Research Foundation, 6411 Ivy Ln Ste 110, Greenbelt, MD, 20770, USA

* darryl.boyd@nrl.navy.mil - 202-404-6140

Supporting Information

Materials:

Sulfur was purchased from All-Chemie Ltd. and distilled as previously described.¹ Tetravinyltin was purchased from Sigma Aldrich and used as received. 1,3-diisopropenyl benzene was purchased from TCI America and used as received. All polymers were fabricated with 0.0095 moles of non-sulfur comonomer.

Methods:

Polymer Fabrication: For the synthesis of poly(S-*r*-DIB), 0.0095 mol (30 wt%) of the DIB comonomer was added to molten sulfur at ~135 °C, and stirred for ~8 min in a Teflon petri dish. The petri dish was then placed in a preheated furnace, and the product cured at 170 °C for 1 hr. Finally, the petri dish was removed from the furnace to allow the ORMOCALC to cool and be extracted in freestanding form. For the synthesis of poly(S-*r*-TVSn), 0.0095 mol TVSn comonomer was added to molten sulfur at 125 – 130 °C, and stirred for 10 – 13 min in a Teflon petri dish. Following the reaction, the petri dish was then moved to a preheated furnace, and the product cured at 125 – 130 °C for 3 – 4 hours. Polymer thicknesses ranged between 1.5 and 1.9 mm, and specific thicknesses are explicitly stated for each analysis within the manuscript and Supporting Information.

Note 1: It is important that all reactions be carried out in ventilated conditions (e.g. in a fume hood). It is also important that reactions be carried out while the researcher is wearing the proper personal protective equipment, including gloves, lab coat and proper eye protection. A respirator, to avoid inhaling any fumes, is also recommended.

Note 2: Successful synthesis of poly(S-*r*-TVSn) using a reaction temperature of ~135 – 140 °C, and a short curing time of ~10 mins has been successfully performed, thus indicating the necessity of careful attention to temperature/timing and consistent fabrication conditions when synthesizing poly(S-*r*-TVSn).

Note 3: Attempts to remelt the poly(S-*r*-TVSn) at temperatures between (100 – 200 °C) were unsuccessful. Attempts to solubilize poly(S-*r*-TVSn) in solvents such as chloroform were inconclusive. Although the polymer lost mass following solubilization attempts, this may be due to the extraction of unreacted reagents within the polymer that would otherwise outgas with time, rather than making a fully reacted poly(S-*r*-TVSn) soluble.

Note 4: The poly(S-*r*-TVSn) is flexible like rubber for several days following fabrication. However, it does gradually stiffen into a non-flexible, yet transparent, solid. Unless otherwise indicated, all of the data reported in the manuscript and Supporting Information was collected shortly after fabrication of the polymer, while the polymer was in a flexible, rubber-like state.

Refractive Index Determination: Refractive index values were determined using a Metricon 2010/M Prism Coupler refractometer, with laser sources at 636.3, 983.6 and 1548.4 nm. The Metricon 2010/M Prism Coupler refractometer utilized a standard Rutile prism whose index was calibrated at each respective wavelength using a reference “Hi-Index” (Schott N-LaF3) glass provided by Metricon. The recorded index values were averaged over five instrument scans.

Spectroscopic Analysis: UV-visible-NIR transmission data was obtained using an Agilent Technologies Cary 7000 Universal Measurement Spectrophotometer in the range of 250 – 2300 nm. FT-IR data was obtained using an Analect Diamond-20 FT-IR, and a Thermo Scientific Nicolet iS50R FT-IR Spectrometer.

Optical Imaging: A digital camera was used to image the polymers in the visible range. SWIR images were taken using a SWIR imager that had an upper limit of 1.3 μm . MWIR images of polymers were taken using a SOFRADIR-EC Model IRE-640BB camera with a 3 – 5 μm lens. LWIR images of polymers were taken using a FLIR T600 Camera in the range of 7.5 – 14 μm .

Differential Scanning Calorimetry Analysis (DSC): DSC was performed on a TA instruments Q200. The reference/control material used for this analysis was an empty aluminum DSC cup, and nitrogen was flowed at 50 ml/min over the sealed cups. The temperature was ramped from -80 to 125 $^{\circ}\text{C}$ at a rate of 5 $^{\circ}\text{C}/\text{minute}$. The glass transition temperatures (T_g) are given in Table 1.

Thermogravimetric Analysis (TGA): TGA was performed on a TA Instruments 2960 SDT. The samples were heated from room temperature to 350 $^{\circ}\text{C}$ at 10 $^{\circ}\text{C}/\text{minute}$ under a nitrogen gas purge. The degradation temperature values given in Table 2 represent the temperature at which 95 mass % and 90 mass % of the sample remained.

X-Ray Diffraction Analysis (XRD): XRD was performed using a Rigaku SmartLab x-ray diffractometer. Samples were measured at room temperature under illumination from a $\text{CuK}\alpha$ x-ray source in a conventional $\theta/2\theta$ geometry. Samples were either measured as an as-synthesized bulk polymer (**Figure S8a**) or as a powder (**Figure S8b**). In order to obtain powder, the bulk polymer was ground in cryogenic temperatures then returned to ambient temperature for analysis.

Additional Figures and Analysis:

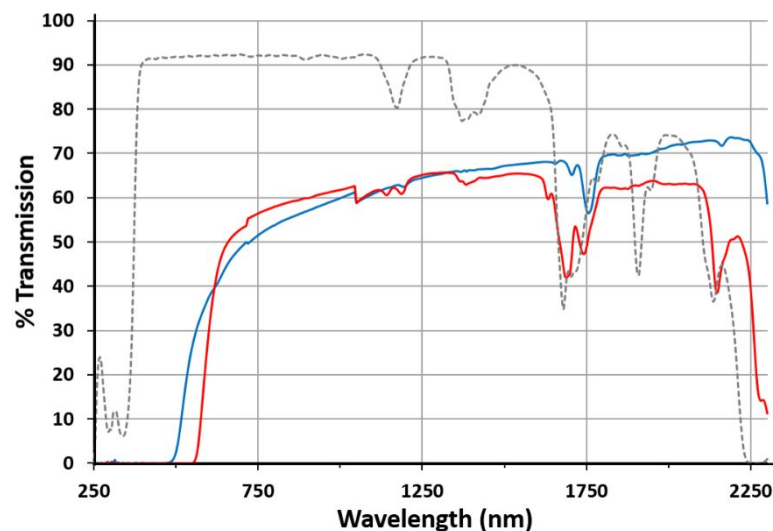


Figure S1. UV-vis-NIR transmission spectra of 1.49 mm thick poly(S-r-TVSn) ORMOCHALC (solid, blue plot), 1.63 mm thick poly(S-r-DIB) ORMOCHALC (solid, red plot), and 1.50 mm thick PMMA (dashed, gray plot).

A comparison of the transmission for PMMA versus the ORMOCHALC polymers poly(S-r-DIB) and poly(S-r-TVSn) in the visible, near-infrared (NIR), and short-wave infrared (SWIR) shows that PMMA has greater transmission for the majority of this region of the electromagnetic spectrum. (**Figure S1**) PMMA transmission drastically decreases beginning at ~1600 nm, ultimately becoming completely opaque at ~2250 nm. Both of the ORMOCHALC polymers

begin to transmit in the visible, with poly(*S-r*-DIB) reaching a maximum of ~65% transmittance at ~1400 nm, and poly(*S-r*-TVSn) consistently increasing to a maximum of ~73% transmittance at ~2200 nm.

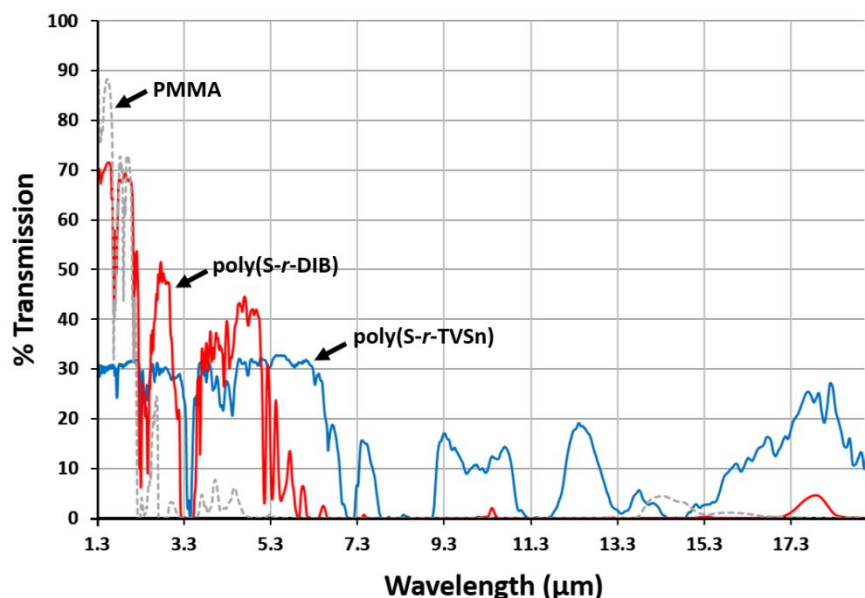


Figure S2. Extended FT-IR transmission spectrum of 1.55 mm thick poly(*S-r*-TVSn) ORMOCALC (solid, blue plot), 1.63 mm thick poly(*S-r*-DIB) ORMOCALC (solid, red plot), and 1.50 mm thick PMMA (dashed, gray plot).

Figure S2 shows the extended FT-IR transmission window of the poly(*S-r*-TVSn) ORMOCALC versus poly(*S-r*-DIB) ORMOCALC and PMMA. PMMA transmission is near zero beyond ~2 μm , while both the poly(*S-r*-TVSn) and poly(*S-r*-DIB) ORMOCALC polymers show substantial transmission in the mid-wave infrared (MWIR) region (3 – 5 μm). However, only the poly(*S-r*-TVSn) ORMOCALC shows substantial transmission in the long-wave infrared (LWIR) region (> 7.5 μm). These FT-IR results agree with the MWIR and LWIR images taken through the polymers, as discussed in the manuscript text. The discrepancy between the percent transmission observed in the UV-vis-NIR analysis (**Figure S1**) versus the FT-IR analysis (**Figure S2**) from ~1300 – 2300 nm is attributed to the difference in thickness of the poly(*S-r*-TVSn) used in each analysis (1.49 mm for UV-Vis vs. 1.65 mm for FT-IR), and the inherent difference in instrumentation detection methods.

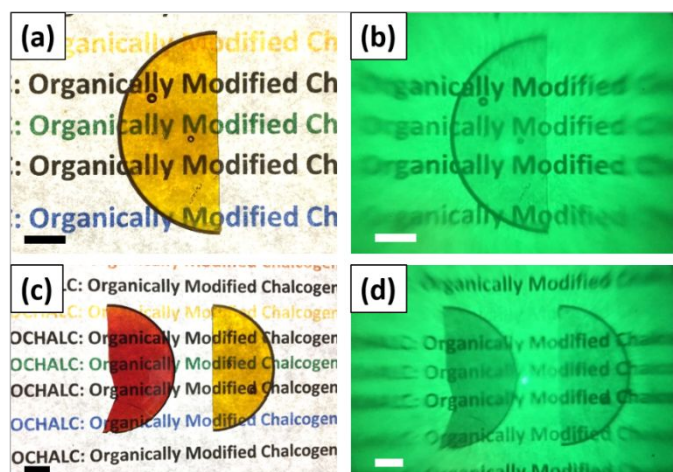


Figure S3. (a) Digital camera image of poly(*S-r*-TVSn), (b) SWIR image of poly(*S-r*-TVSn), (c) comparative digital camera image of poly(*S-r*-DIB) vs. poly(*S-r*-TVSn), (d) SWIR image of poly(*S-r*-DIB) vs. poly(*S-r*-TVSn). Poly(*S-r*-TVSn) and poly(*S-r*-DIB) shown are 1.65 mm and 1.63 mm thick, respectively. Scale bars = 1 cm.

As described in the manuscript, poly(*S-r*-TVSn) ORMOCALC polymers appear light brown to brown in color, depending on the thickness. (**Figure S3**) This is in contrast to poly(*S-r*-DIB), which appears red to deep red in color. (**Figure S3c**) As expected, given the FT-IR analysis, both poly(*S-r*-DIB) and poly(*S-r*-TVSn) are transparent in the NIR and the SWIR. (**Figure S3b,d**)

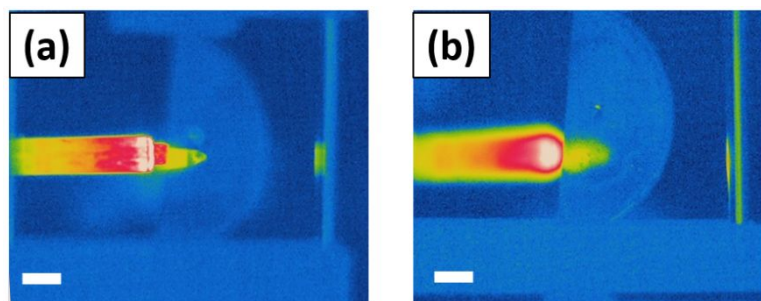


Figure S4. LWIR image showing the transparency of poly(*S-r*-TVSn) (a) with the soldering iron in focus, and (b) with the poly(*S-r*-TVSn) ORMOCALC polymer in focus. The poly(*S-r*-TVSn) ORMOCALC shown is 1.65 mm in thickness. Scale bars = 1 cm.

Figure S4 shows the LWIR transparency of the poly(*S-r*-TVSn) ORMOCALC polymer with the object being imaged in focus, versus the surface of the polymer itself being in focus. Both images clearly demonstrate the transparency of the poly(*S-r*-TVSn) ORMOCALC in the LWIR.

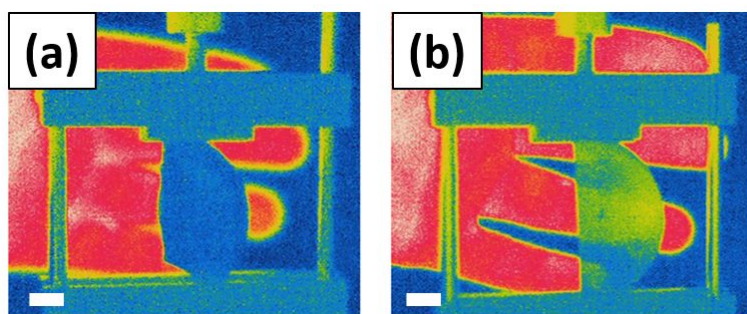


Figure S5. LWIR image showing (a) the opacity of 1.63 mm thick poly(*S-r*-DIB), and (b) the transparency of 1.65 mm thick poly(*S-r*-TVSn). Scale bars = 1 cm.

Figure S5a clearly demonstrates that the poly(*S-r*-DIB) polymer does not transmit (i.e. is opaque) in the LWIR. Poly(*S-r*-DIB) appears as a ‘cold-body’ object, not allowing the warm human fingers to be seen through the polymer. By contrast, Figure S5b shows the LWIR transparency of the poly(*S-r*-TVSn) ORMOCALC polymer with the warm fingers being distinguishable through the polymer.

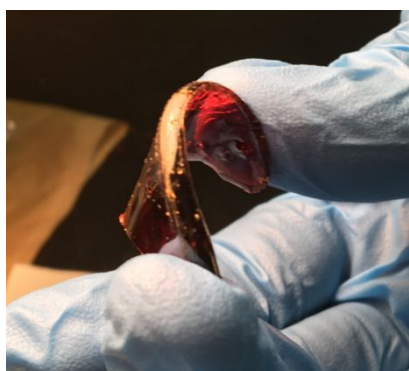


Figure S6. Image showing the flexibility of poly(S-*r*-TVSn).

Figure S6 shows a poly(S-*r*-TVSn) ORMOCHALC polymer being bent shortly after fabrication. Figure S6 also shows the brown, yet transparent, color of the ORMOCHALC. Although initially flexible upon fabrication, each poly(S-*r*-TVSn) ORMOCHALC eventually stiffens, and is no longer flexible.

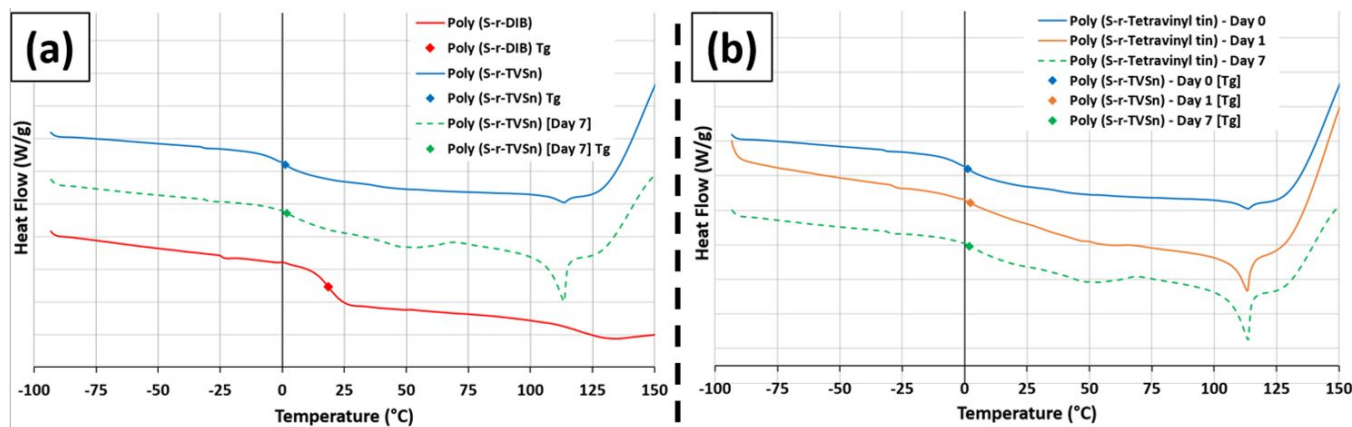


Figure S7. (a) Differential Scanning Calorimetry (DSC) data indicating the glass transition temperatures (T_g) for poly(S-*r*-DIB), poly(S-*r*-TVSn), and poly(S-*r*-TVSn) after 7 days. (b) DSC data for poly(S-*r*-TVSn) various days after fabrication.

Differential Scanning Calorimetry (DSC) was employed to determine any phase changes in the material. The results show that the stiffer poly(S-*r*-DIB) had a greater glass transition temperature (~20 °C) than the rubbery poly(S-*r*-TVSn) (~1 °C). (Figure S7a) This result might be expected, as poly(S-*r*-TVSn) was qualitatively rubbery upon fabrication. However, despite stiffening by the 7th day following fabrication, Figure S7b shows that the T_g for poly(S-*r*-TVSn) only increased by less than 1 °C. Figure S7b indicates the presence of a small amount of unreacted sulfur within the polymer upon fabrication (Day 0), as indicated by the small trough at ~115 °C. This small trough substantially increased after only 1 day (Day 1). Although the polymer was stiff by Day 7, the unreacted sulfur-related DSC trough had not significantly increased from Day 1 to Day 7, suggesting that the polymer was reaching internal stability.

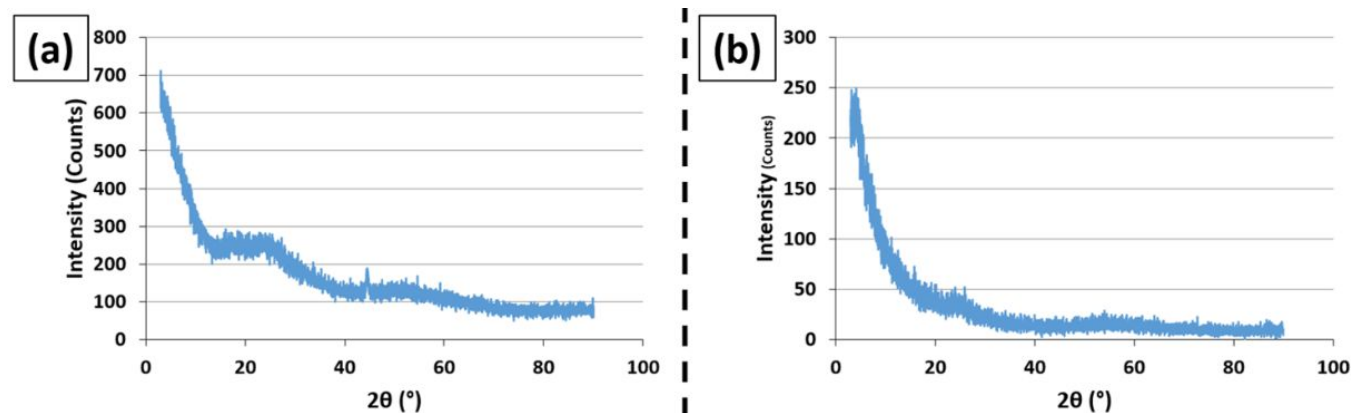


Figure S8. (a) X-Ray Diffraction and (b) powder X-Ray Diffraction data plots for poly(S-*r*-TVSn).

Due to the sulfur trough being present in the DSC data (Figure S7), it was necessary to determine whether crystallization was occurring within the poly(S-*r*-TVSn) as the polymer stiffened in the days following fabrication. Figure S8a shows X-Ray Diffraction (XRD) data for 2-day-old poly(S-*r*-TVSn), and Figure S8b shows powder X-Ray

Diffraction (PXRD) data for 7-day-old poly(S-*r*-TVSn). While XRD analysis is limited by the depth within a material at which it can detect crystals, PXRD allows much easier detection of crystals. The lack of any sharp peaks in either the XRD or the PXRD data suggests that the poly(S-*r*-TVSn) is amorphous, and contains few areas of crystallization (if any at all).(**Figure S8**)

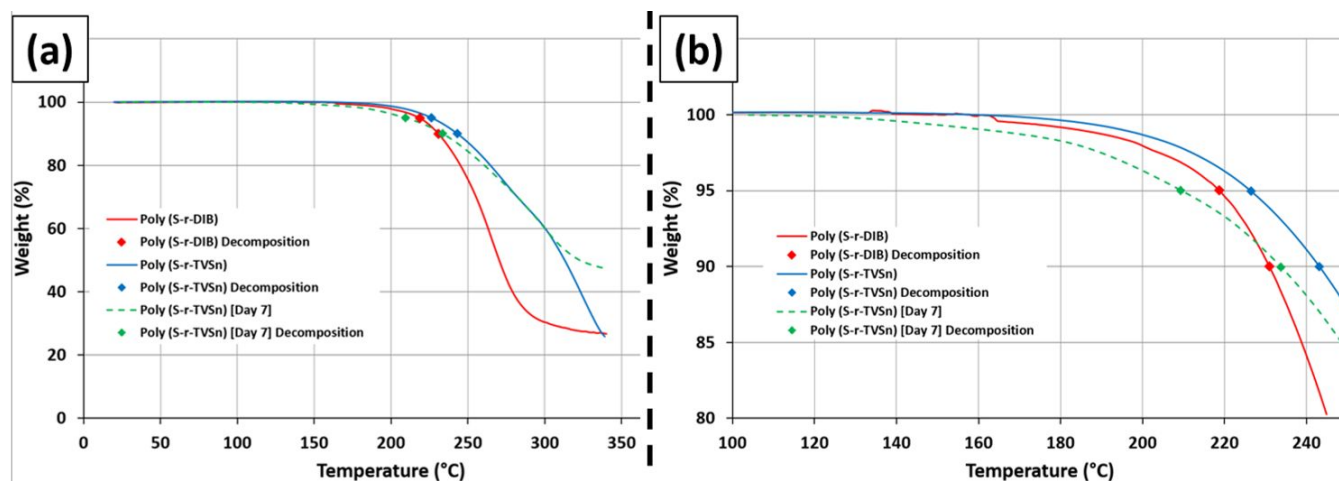


Figure S9. (a) Complete and (b) zoomed-in Thermal Gravimetric Analysis (TGA) data for poly(S-*r*-DIB), poly(S-*r*-TVSn), and poly(S-*r*-TVSn) after 7 days.

TGA analysis shows the degradation temperature of poly(S-*r*-TVSn) to be similar to that of poly(S-*r*-DIB) when less than 10 % of the mass has been burned off.(**Figure S9**) However, there is great divergence in the degradation behavior between the two polymers as temperature increases beyond 250 °C.(**Figure S9a**) The degradation behavior of 7-day-old poly(S-*r*-TVSn) also diverges greatly from that of ‘freshly made’ poly(S-*r*-TVSn) at temperatures beyond ~300 °C.(**Figure S9a**)

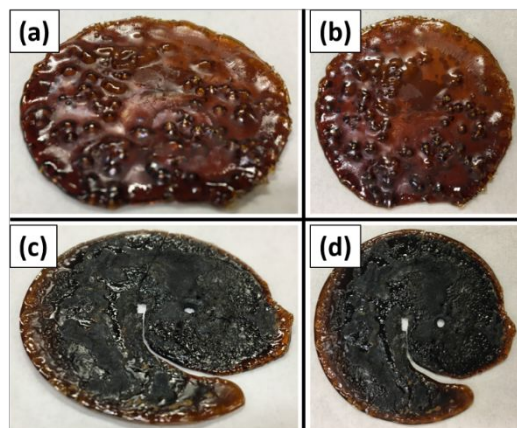


Figure S10. Tilted (a) & (c), and top-down (b) & (d) images of poorly processed poly(S-*r*-TVSn) ORMOCHALC polymers.

Fabrication of poly(S-*r*-TVSn) requires careful attention to how long the reaction is carried out, what temperature it is carried out at, how long it is cured, and the temperature at which it is cured. These factors likely vary depending on the instrumentation and molds being used. Figures S10a & S10b show an example of when a poly(S-*r*-TVSn) is cured in the furnace for too long. Figures S10c & S10d show an example of when the poly(S-*r*-TVSn) reaction is performed for too long (prior to curing in the furnace). During some instances, when the reaction is carried out for too long, rapid decomposition of the product has been observed to happen in almost a chain-like

fashion; beginning at one side of the polymer and progressing to a different side of the polymer in a few seconds, leaving behind a charred material as it goes. It is likely that toxic gases do form when the polymer decomposes in this fashion, as smoke evolves from the product as it decomposes.

REFERENCE

1. Boyd, D. A.; Baker, C. C.; Myers, J. D.; Nguyen, V. Q.; Drake, G. A.; McClain, C. C.; Kung, F. H.; Bowman, S. R.; Kim, W.; Sanghera, J. S. ORMOCALCs: Organically Modified Chalcogenide Polymers for Infrared Optics. *Chem. Commun.* **2017**, 53 (1), 259-262.